Supporting Information

Hydrotrope Induced Structural Modifications in CTAB/Butanol/Water/Isooctane Reverse Micellar System

Vaishali Sethi[1], Jayanti Mishra[1], Arpan Bhattacharayya[2], Debasis Sen[3] and Ashok K. Ganguli*[1, 4]

1. Department of Chemistry, Indian Institute of Technology, Hauz Khas, New Delhi-110016, India.

2. Surface Physics and Material Science Division, Saha Institute of Nuclear Physics, Kolkata-700064, India.

3. Solid State Physics Division, Bhabha Atomic Research Centre, Mumbai 400085, India.

4. Institute of Nano Science & Technology, Habitat Centre, Phase- X, Sector – 64, Mohali, Punjab–160062, India.

Contents

1. Scheme 1

2. Volume fraction of micellar systems.

3. Structural parameters of hydrotrope- based CTAB reverse micellar system.

4. Parameters obtained from model fits of scattering data at different water loadings.

5. Schematic of structural transitions in hydrotrope-based reverse micellar system.

6. ^{1}H Chemical shift data for hydrotrope-based CTAB reverse micellar solutions at different W_x value

7. ^{1}HNMR spectrum of W_{16} and W_{20} reverse micellar system.

8. Experimental section.

9. Model Independent analysis of SAXS data.

10. References

Scheme 1: Molecular structure and nomenclature of the protons of different components of reverse micellar system for ^{1}HNMR investigations (a) CTAB (b) Sodium salicylate (c) Isooctane (d) Butanol

(a)

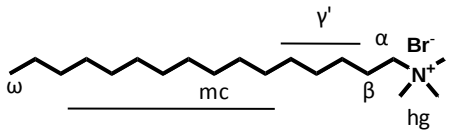

(b)

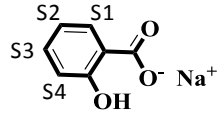

(c)

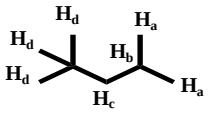

(d)

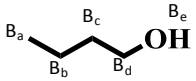

2. Volume fraction of micellar systems obtained from density- measurements

TABLE S1: Density of hydrotrope-based reverse micellar solutions at different water loadings.

	Density (in g/cm^3)				
R	W_4	W_{12}	W_{16}	W_{20}	W_{30}
R_0	0.7601	0.7718	0.7798	0.7830	0.7964
$R_{0.2}$	0.7680	0.7791	0.7859	0.7895	0.8013
$R_{0.4}$	System unstable	0.7835	0.7840	0.7947	0.8068
$R_{0.6}$	System unstable	0.7895	0.7959	0.8006	0.8120
$R_{0.8}$	System unstable	0.7947	0.8028	0.8049	0.8179
R_1	System unstable	0.7955	0.8064	0.8105	0.8219

TABLE S2: Volume fraction of hydrotrope-based reverse micellar solutions calculated from density measurement.

R	W_4	W_{12}	W_{16}	W_{20}	W_{30}
R_0	0.1208	0.1794	0.2027	0.2349	0.3075
$R_{0.2}$	0.1092	0.1687	0.1938	0.2254	0.2900
$R_{0.4}$	–	0.1624	0.1865	0.2179	0.2924
$R_{0.6}$	–	0.1537	0.1792	0.2093	0.2847
$R_{0.8}$	–	0.1460	0.1692	0.2030	0.2763
R_1	–	0.1390	0.1639	0.1949	0.2704

TABLE S3: Structural parameters of selected CTAB reverse micellar system obtained from complete fit of SAXS curve using cylindrical/ prolate ellipsoidal form factor and PRISM/Macroion as structure factor at different water loadings (W_x).

			W_4			
R	**radius (nm)**	**length (nm)**	**v_{mic} (nm^3)**	**N_{H2O}**	**N_{CTAB}**	**$N_{micelles}$ (10^{16})**
R_0	1.09	32	119.38	3979	11937	5.38
$R_{0.2}$	1.03	48	186.55	6218	24872	2.59

R	**a (nm)**	**c (nm)**	**R_w (nm)**	**v_{mic} (nm^3)**	**N_{H2O}**	**N_{CTAB}**	**$N_{micelles}$ (10^{16})**	**α_f**	**A_w (nm^2)**
				W_{12}					
R_0	1.60	7.91	2.7	82	2400	200	320	0.0053	92
$R_{0.2}$	1.65	14.02	3.3	150	4392	366	170	0.0048	137
$R_{0.4}$	1.80	17.50	3.8	229	6708	559	110	0.0032	181
$R_{0.6}$	1.74	19.02	4.0	267	7836	653	100	0.0026	201
R_1	1.77	31.51	4.6	407	11940	995	62	0.0017	266
				W_{16}					
R_0	1.95	9.07	3.4	145	4384	274	230	0.0040	145
$R_{0.2}$	2.00	16.2	4.0	277	8384	524	120	0.0035	200
$R_{0.4}$	2.00	20.03	4.3	338	10224	639	100	0.0033	232
$R_{0.6}$	1.96	24.20	4.5	382	11552	722	89	0.0030	254
$R_{0.8}$	1.95	29.31	4.8	466	14096	881	73	0.0025	289
R_1	1.89	37.81	5.1	571	17264	1079	62	0.0016	326
				W_{20}					
R_0	2.36	20.01	4.8	466	14360	718	90	0.0016	289
$R_{0.2}$	2.56	23.61	5.3	647	19940	997	63	0.0015	352
$R_{0.4}$	2.56	30.06	5.8	823	25360	1268	51	0.0013	422
$R_{0.6}$	2.61	32.50	6.0	926	28540	1427	45	0.0013	452
$R_{0.8}$	2.58	34.20	6.1	947	29180	1459	44	0.0012	467
R_1	2.70	38.33	6.6	1194	36800	1840	35	0.0009	547
				W_{30}					
R_0	3.20	16.60	5.5	749	22470	790	86	0.0026	379
$R_{0.2}$	3.41	21.41	6.2	1090	32700	1150	59	0.0022	482
$R_{0.4}$	3.40	23.83	6.5	1213	36390	1278	53	0.0020	530
$R_{0.6}$	3.42	26.12	6.7	1331	39930	1403	48	0.0019	563
$R_{0.8}$	3.40	28.51	6.9	1453	43590	1532	44	0.0017	597

TABLE S4: Parameters obtained from model fits for W_4 CTAB reverse micellar system at different ±hydrotrope concentration considering PRISM structure factor.

	FORM FACTOR CYLINDRICAL		STRUCTURE FACTOR PRISM			
	radius (nm)	length (nm)	radius (nm)	length (nm)	osmotic compressibility	χ^2
R_0	1.09 ± 0.01	32±1	1.08	8	2.8	1.87
$R_{0.2}$	1.03 ±0.01	48±2	1.08	8	3.2	2.07

TABLE S5: Parameters obtained from model fits for W_{12} CTAB reverse micellar system at different hydrotrope concentration

	FORM FACTOR ELLIPSOID II				STRUCTURE FACTOR MACRO ION					
R	a	c	nu	Eta	Z	RHS	ION	η	Vf	χ^2
R_0	1.60 ±0.01	7.91	4.95 ±0.06	0.0209 ±0.0001	0.455 ±0.001	3.10 ±0.01	0.352	0.1794	0.1794	1.74
$R_{0.2}$	1.65 ±0.02	14.02	7.73 ±0.19	0.0187 ±0.0002	2.019 ±0.001	2.60 ±0.01	0.422	0.1687	0.1687	2.4
$R_{0.4}$	1.80 ±0.01	17.50	9.73 ±0.12	0.0145 ±0.0005	2.036 ±0.008	2.64 ±0.02	0.492	0.1623	0.1623	3.1
$R_{0.6}$	1.74 ±0.02	19.02	11.12 ±0.65	0.0140 ±0.0004	1.918 ±0.009	2.72 ±0.03	0.563	0.1536	0.1536	4.9
R_1	1.77 ±0.03	31.15	17.81 ±0.30	0.0116 ±0.0001	1.932 ±0.008	2.51 ±0.02	0.724	0.1390	0.1390	3.9

a = minor axis of ellipsoid (nm)
c = major axis of ellipsoid (nm)
Eta = scattering constant
ION= Ionic strength
nu = c/a
Z = charge on reverse micellar system
RHS = Radius of Hard sphere interaction (in nm)
η = Volume fraction obtained from fit
V_f = Volume fraction obtained from density measurement
χ^2 = Reduced chi-square

TABLE S6: Parameters obtained from model fits for W_{16} CTAB reverse micellar system at different hydrotrope concentration

	FORM FACTOR ELLIPSOID II				STRUCTURE FACTOR MACRO ION					
R	a	c	nu	Eta	Z	RHS	ION	η	Vf	χ^2
R_0	1.95 ±0.04	9.07	4.65 ±0.27	0.0155 ±0.0004	1.213 ±0.014	3.74 ±0.01	0.352	0.2027	0.2027	3.2
$R_{0.2}$	2.00 ±0.03	16.2	8.05 ±0.36	0.0117 ±0.0002	1.914 ±0.016	3.49 ±0.07	0.422	0.1938	0.1938	2.3
$R_{0.4}$	2.02 ±0.04	20.03	10.23 ±0.25	0.0115 ±0.0002	2.323 ±0.011	3.06 ±0.06	0.492	0.1879	0.1879	3.0
$R_{0.6}$	1.95 ±0.05	24.20	12.24 ±0.55	0.0118 ±0.0003	2.397 ±0.009	3.04 ±0.05	0.563	0.1792	0.1792	4.7
$R_{0.8}$	1.95 ±0.03	29.31	15.01 ±0.23	0.0111 ±0.0003	2.44 ±0.007	2.87 ±0.05	0.634	0.1692	0.1692	3.9
R_1	1.89 ±0.02	37.81	20.02 ±0.20	0.0104 ±0.0002	2.011 ±0.009	2.92 ±0.06	0.704	0.1639	0.1639	5.5

TABLE S7: Parameters obtained from model fits for W_{20} CTAB reverse micellar system at different hydrotrope concentration

	FORM FACTOR ELLIPSOID II				STRUCTURE FACTOR MACRO ION					
R	a	c	nu	Eta	Z	RHS	ION	η	Vf	χ^2
R_0	2.38	20.01	8.40	0.0088	1.210	3.78	0.292	0.1671	0.2349	1.8
	±0.08		±0.21	±0.0007	±0.014	±0.02		±0.005		
$R_{0.2}$	2.59	23.61	9.1	0.0069	2.172	4.47	0.404	0.2048	0.2254	1.7
	±0.01		±0.15	±0.0006	±0.024	±0.01		±0.004		
$R_{0.4}$	2.58	30.06	11.62	0.0072	1.925	4.06	0.454	0.2069	0.2179	1.5
	±0.02		±0.43	±0.001	±0.026	±0.01		±0.005		
$R_{0.6}$	2.68	32.50	12.10	0.0062	2.414	3.83	0.523	0.1923	0.2093	1.9
	±0.03		±0.11	±0.0004	±0.011	±0.05		±0.003		
$R_{0.8}$	2.56	34.20	13.32	0.0070	1.871	3.66	0.582	0.1908	0.2030	1.9
	±0.02		±0.61	±0.0001	±0.009	±0.04		±0.006		
R_1	2.73	38.33	14.01	0.0058	1.9140	3.65	0.600	0.1848	0.1949	2.3
	±0.04		±0.41	±0.0002	±0.023	±0.06		±0.004		

TABLE S8: Parameters obtained from model fits for W_{30} CTAB reverse micellar system at different hydrotrope concentration

	FORM FACTOR ELLIPSOID II				STRUCTURE FACTOR MACRO ION					
R	a	c	nu	Eta	Z	RHS	ION	η	Vf	χ^2
R_0	3.14	16.60	5.28	0.0061	2.045	4.92	0.296	0.1852	0.3075	1.5
	±0.09		±0.21	±0.0004	±0.097	±0.03		±0.004		
$R_{0.2}$	3.41	21.41	6.31	0.0055	2.585	5.19	0.173	0.2240	0.2973	1.5
	±0.06		±0.11	±0.0003	±0.018	±0.02		±0.003		
$R_{0.4}$	3.42	23.83	7.01	0.0054	2.593	5.08	0.513	0.2289	0.2924	1.4
	±0.09		±0.18	±0.0003	±0.204	±0.03		±0.006		
$R_{0.6}$	3.42	26.12	7.61	0.0052	2.750	5.08	0.546	0.2281	0.2846	1.5
	±0.05		±0.16	±0.0002	±0.145	±0.02		±0.002		
$R_{0.8}$	3.40	28.51	8.42	0.0056	2.624	5.09	0.645	0.2278	0.2762	1.2
	±0.01		±0.19	±0.0004	±0.181	±0.09		±0.005		

TABLE S9: Scattering length densities of different components of reverse micelle.

	X-ray(10^{-6}/Å^2)
Isooctane	**6.80**
H_2O	**9.47**
$C_{19}H_{42}N$	**6.82**
OHC_6H_4COONa	**3.93**
Butanol	**7.81**
Br^-	**26.61**

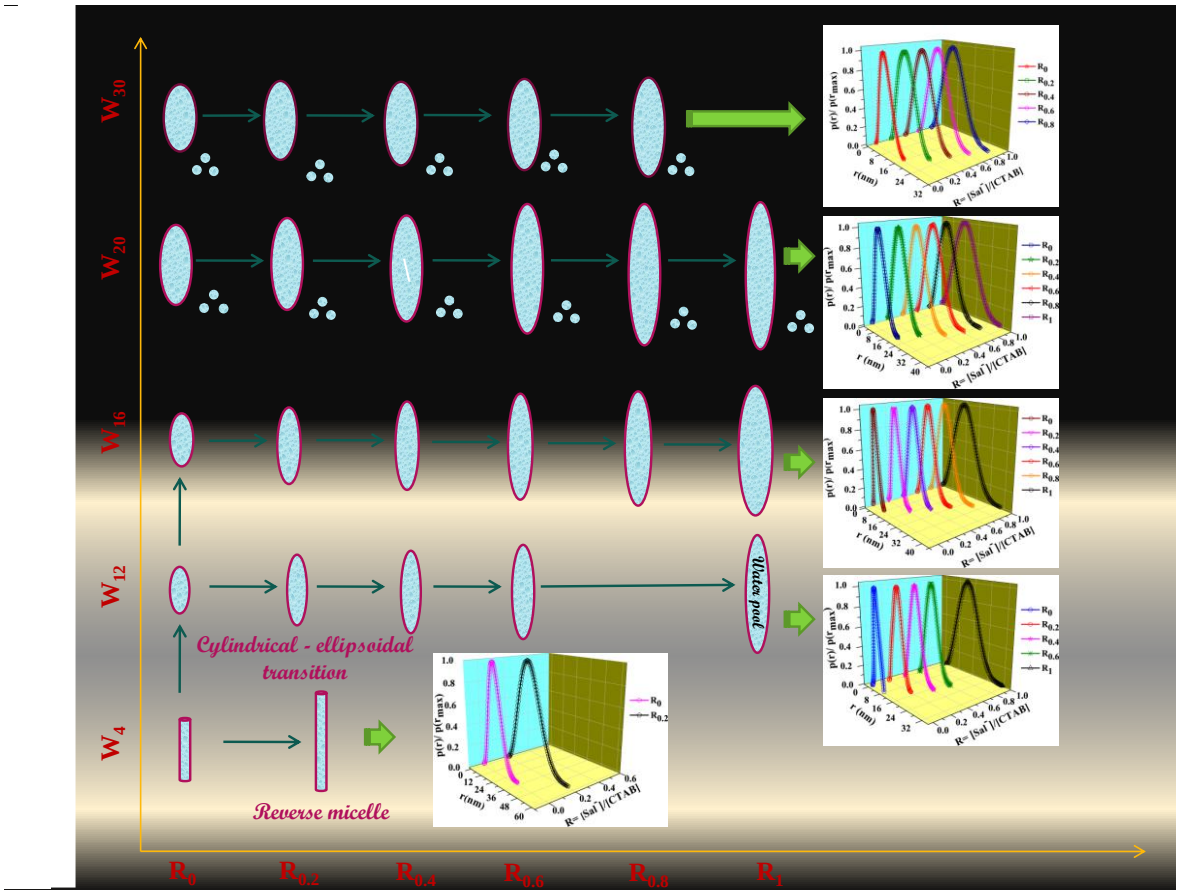

Figure S1: Schematic representation of cylindrical to ellipsoidal transition and hydrotrope induced micellar growth in CTAB microemulsion system at different water loadings.

Table S10. ^{1}H Chemical shift data for hydrotrope-based CTAB reverse micellar solutions at different W_x value

Solutions	α	hg	β	γ'	mc'	Ω	S1	S3	S2/S4	α - but	B_w	I_w
100mm CTAB	3.62	3.48	1.76	1.37	1.26	0.88						
NaSal in D_2O							8.24 (d)	7.49 (t)	6.82 (q)			
						W_4						
R_0	3.78	3.57	2.05			1.05				3.85	4.64	5.06
$R_{0.2}$	3.70	3.54	2.01			1.04	8.14	7.46	7.05	3.83	4.74	D
						W_{12}						
R_0	3.70	3.49	2.08			1.03				3.84	4.83	5.16
$R_{0.2}$	3.63	3.46	2.01			1.02	8.15	7.44	7.03	3.82	4.82	5.11
$R_{0.4}$	3.55	3.42				1.01	8.13	7.43	7.02	3.80	4.82	D
$R_{0.6}$	3.46	3.38				1.00	8.11	7.41	7.00	3.78	4.82	D
$R_{0.8}$	3.38	3.33				1.00	8.09	7.39	6.98	3.76	4.81	D
R_1	3.32	3.29				0.99	8.07	7.37	6.96	3.74	4.81	D
						W_{16}						
R_0	3.70	3.48	2.0			1.02				3.84	4.88	5.15
$R_{0.2}$	3.61	3.44	2.00			1.00	8.13	7.43	7.02	3.81	4.86	5.11
$R_{0.4}$	3.53	3.40				0.99	8.11	7.42	7.00	3.78	4.86	D
$R_{0.6}$	3.44	3.36				0.99	8.09	7.40	6.99	3.77	4.84	D
$R_{0.8}$	3.36	3.31				0.99	8.07	7.38	6.97	3.75	4.84	D
R_1	3.31	3.27				0.98	8.06	7.36	6.96	3.74	4.82	D
						W_{20}						
R_0	3.64	3.42	2.04			0.97				3.79	4.90	5.17
$R_{0.2}$	3.60	3.42	2.00			0.99	8.13	7.43	7.02	3.80	4.88	5.13
$R_{0.4}$	3.51	3.39				0.99	8.11	7.42	7.00	3.78	4.87	D
$R_{0.6}$	3.43	3.34				0.99	8.08	7.40	6.98	3.75	4.86	D
$R_{0.8}$	3.35	3.30				0.98	8.07	7.38	6.96	3.74	4.85	D
R_1	3.29	3.25				0.97	8.04	7.38	6.94	3.72	4.83	D
						W_{30}						
R_0	3.65	3.41	2.10							3.80	4.93	5.18
$R_{0.2}$	3.55	3.40	1.98				8.09	7.40	6.98	3.77	4.91	5.15
$R_{0.4}$	3.47	3.39					8.07	7.38	6.97	3.75	4.90	5.13
$R_{0.6}$	3.45	3.39					8.07	7.39	6.97	3.75	4.89	5.12
$R_{0.8}$	3.40	3.38					8.06	7.38	6.97	3.75	4.89	5.09

D= Peak Disappeared

Table S11. Comparative trends of V_{Na+} and V_{mic} for W_{12} and W_{30} system at different R values

R value	Number density of Na^+ ions at different salicylate concentration $[ND_{Na+}]$	Number of sodium ions per micelle $N_{Na+} = [ND_{Na+}/N_m]$	Total Volume of Na^+ ions per micelle $V_{Na+} = [v_{Na+} * N_{Na+}]$ (nm^3)	Volume of ellipsoidal micelle (nm^3)
W_{12}				
$R_{0.2}$	$1.28*10^{20}$	75	0.68	150
$R_{0.4}$	$2.6*10^{20}$	236	2.12	229
$R_{0.6}$	$3.9*10^{20}$	390	3.51	267
R_1	$6.5*10^{20}$	1083	9.75	407
W_{30}				
$R_{0.2}$	$1.28*10^{20}$	148	1.33	1035
$R_{0.4}$	$2.6*10^{20}$	509	4.58	1151
$R_{0.6}$	$3.9*10^{20}$	736	6.62	1263
$R_{0.8}$	$5.2*10^{20}$	1181	10.63	1379

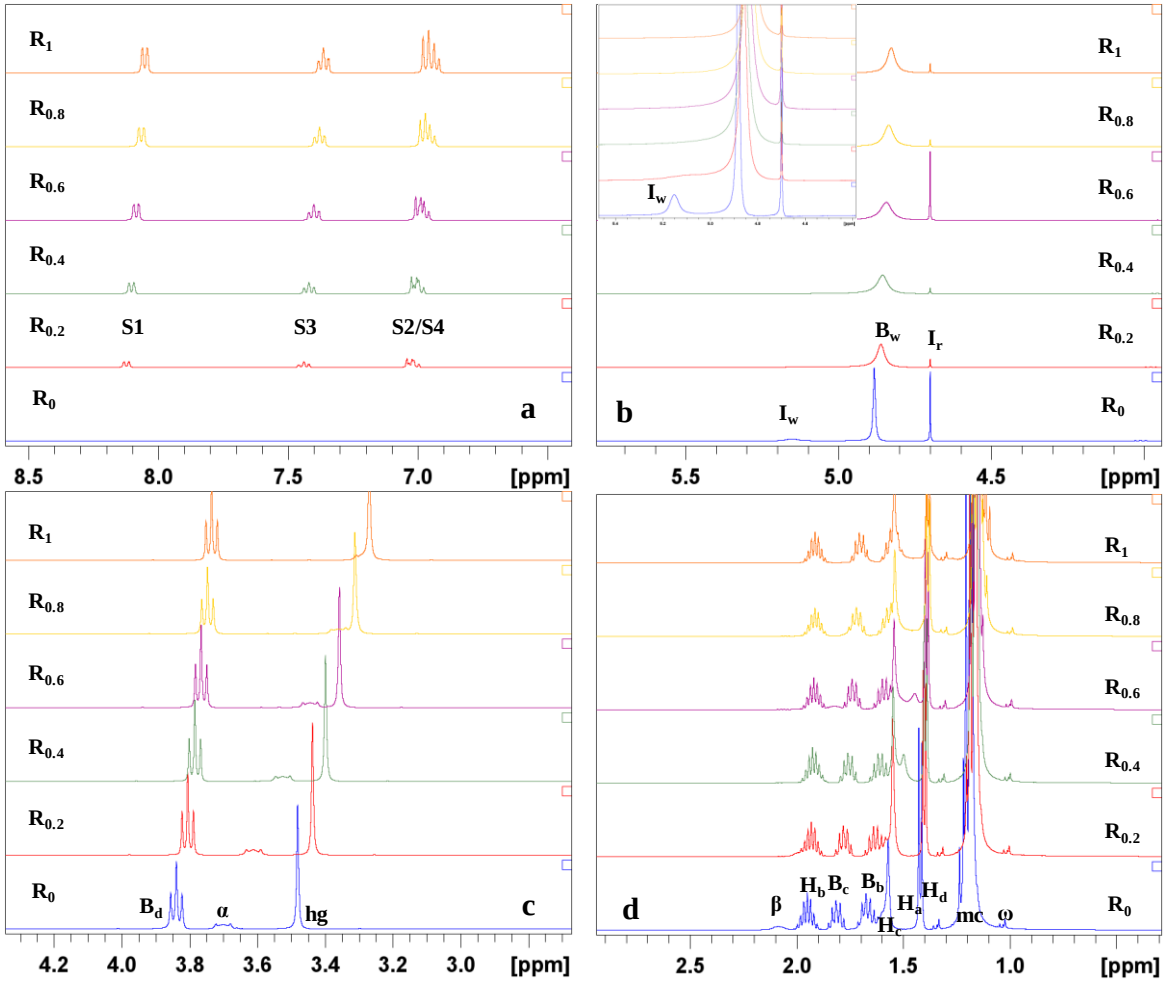

Figure S2**.** Different regions of ^{1}HNMR spectrum of W_{16} reverse micellar systems at different R values (a) aromatic salicylate protons (b) interfacial and bulk water proton resonance peak (c) resonance of B_d and α , hg protons of co-surfactant and surfactant respectively (d)Protons corresponding to hydrophobic tails of surfactant , co-surfactant and organic isooctane layer.

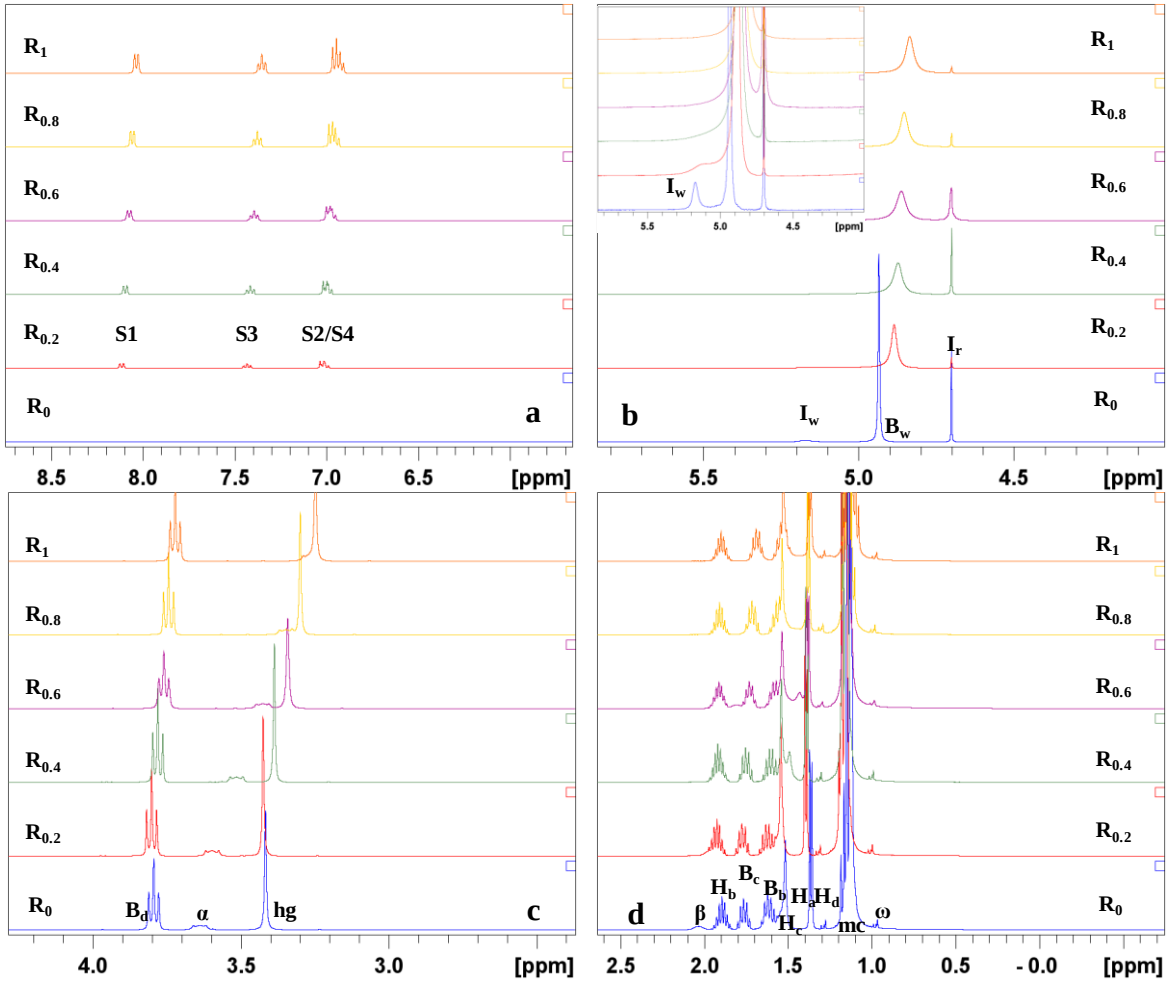

Figure S3**.** Different regions of ^{1}HNMR spectrum of W_{20} reverse micellar systems at different R values (a) aromatic salicylate protons (b) interfacial and bulk water proton resonance peak (c) resonance of B_d and α , hg protons of co-surfactant and surfactant respectively (d)Protons corresponding to hydrophobic tails of surfactant , co-surfactant and organic isooctane layer.

Density Measurement

The densities of the organic solvent isooctane (ρ_{oil}) and of reverse micellar solutions (ρ_s) at different salt concentration were determined at 25.00 ± 0.01°C using DE45 Mettler Toledo density meter. For each solution the density measurement were performed atleast 3 times and averaged. The precision obtained is of the order of ± $2*10^{-4}$ g/cm^3.

Small - Angle X-ray Scattering Measurement: SAXS measurements were conducted at the Indian Beamline at 2.5GeV second generation synchrotron at Photon Factory, KEK, Japan, with a custom designed SAXS setup. The geometry used for the experiment was transmission mode SAXS, sample was kept in a custom made glass capillary (1.5 mm diameter) on a custom made holder and was illuminated using a monochromatic X-Ray of energy 10KeV with a sample to detector distance of 3902mm. The beam dimension used was 0.4 mm vertically and 1mm horizontally. The 2-D scattering pattern was recorded by 1M PILATUS detector with a pixel resolution of 172µm X 172µm with total number of pixels to be 981 X 1043 for Vertical X Horizontal geometry. The 2D raw data was linearly averaged with GIXSGUI programme[1] written on MATLAB and obtained as one - dimensional scattering intensities, I (q), as a function of the scattering vector $[q = 4\pi/\lambda \sin \theta/2]$ where θ corresponds to scattering angle. For our experiments the maximum and minimum dimensions probed by scattered rays are 57nm & 3.5 nm respectively (corresponding to q-range of 0.13 to 1.78 nm^{-1}).The 1D scattering intensity distribution, I (q), were corrected for background and capillary effect contributions and represented in arbitrary unit.[2] All scattering curves were analyzed by the Indirect Fourier transformation using the program ScÅtter to calculate PDDF and also fitted with standard scattering models using SASFIT.[3]

Proton Nuclear Magnetic Resonance (^{1}H NMR)

The ^{1}H NMR spectra of reverse micellar system corresponding to 6 different R value (R_0-R_1) for each targeted W_x value had been recorded with the help of Bruker Avon 400 MHz spectrometer (at Indian Institute of Technology Delhi) at 25° C. The chemical shift of ^{1}H protons are represented in ppm and calibrated with an external standard. The external standard used was a reference capillary filled with D_2O having chemical shift of δ = 4.7 ppm and added in the NMR

tube of each microemulsion system prior to the measurement. Number of scans for all ^{1}H NMR measurements were kept constant i.e. 48.

Model Independent analysis of SAXS data

The SAXS scattering curves were also evaluated by Indirect Fourier transformation[4] (IFT) using ScÅtter software which works on modifications of Moore function[5] to convert the scattering data into real space and to determine the pair-distance distribution function, p(r). The shape and maximum dimension of the particle, r_{max} (abscissa value where p(r) reaches zero) are the two important parameters which can be estimated from p(r) curves.

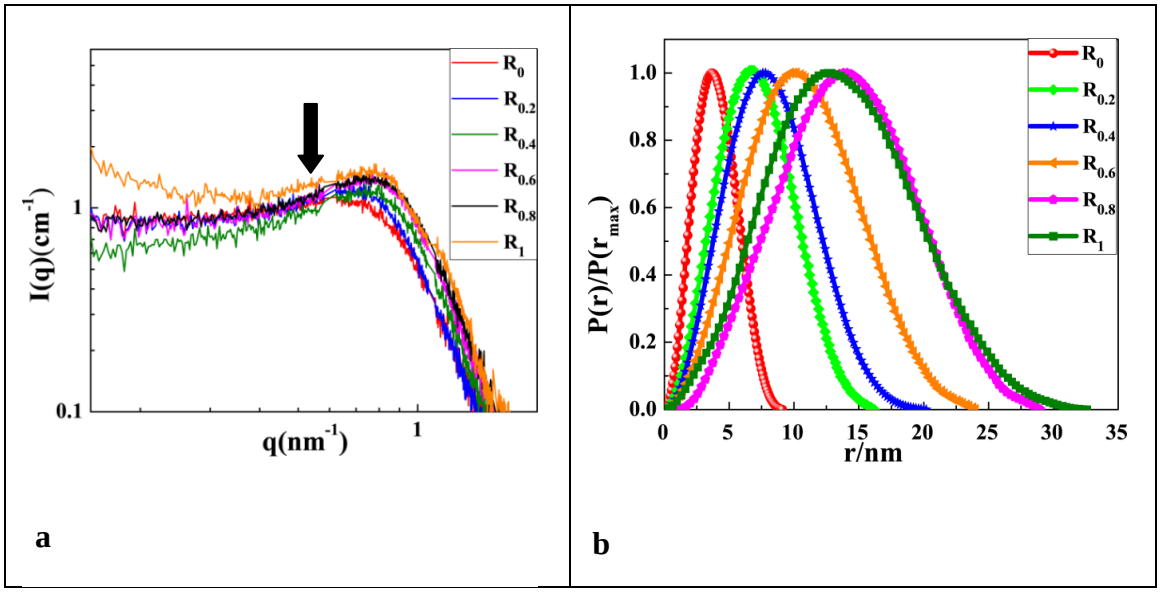

Figure S4. (a) Scattering profile for W_{16} (b) Corresponding normalized pair density distribution function $p(r)/p(r_{max})$ as a function of maximum dimension of ellipsoid r(nm)

The IFT transformation is performed on the scattering profile after trimming the intensity points upto the q-value corresponding to the highest intensity of each scattering curve (represented by arrow in Figure S4 (a)) below which the intensity decreases abruptly due to extensive intermicellar interaction) and by increasing the r_{max} (nm) value to obtain the positive p(r) distribution . The r_{max} (representing the major axis of the ellipsoid) and shape of the particle obtained from p(r) curves are in good agreement with that obtained from model fits for all the W_x value studied. Figure S4 (a) & (b) represents the scattering profile and normalized pair distance distribution function p(r) for systems with water loadings W_{16}. Details regarding the p(r) functions of the other reverse micellar systems studied at different W_x value are given in the

main manuscript, however the similar procedure (as described above) is followed for calculation of p(r) function for other systems also.

References:

1 Z. Jiang, *J. Appl. Crystallogr.*, 2015, **48**, 917–926.
2 T. Zemb, O. Tache, F. Né and O. Spalla, *J. Appl. Crystallogr.*, 2003, **36**, 800–805.
3 I. Breßler, J. Kohlbrecher and A. F. Thünemann, *J. Appl. Crystallogr.*, 2015, **48**, 1587–1598.
4 O. Glatter, *J. Appl. Crystallogr.*, 1979, **12**, 166–175.
5 P. B. Moore, *J. Appl. Crystallogr.*, 1980, **13**, 168–175.